NOVEL USES FOR TIRE PYROLYSIS CHAR

William Petrich

United Carbon Corporation

KEYWORDS: Carbon black, char, pyrolysis

Introduction

Char produced from the thermal conversion of used automobile tires contains a blend of the carbon blacks used in the manufacture of the tire as well as "ash" constituents formed in the pyrolitic process. This mixture provided a challenge to determine possible secondary and tertiary uses. Early work attempted to separate the "ash" fraction from the carbon black species.(1). Subsequent effort uncovered the relationship between the carbon black and the ash fractions and suggested a reverse method of formulation. Because all of the materials found in the char were derived from the recipes used in building the tread, side-wall and bead of the tire, it was anticipated that these materials, in ratio, could be used for other blended engineering materials. The idea of using the char as a "basic" starting material for formulated chemical specialties outside of the rubber industry was supported by two factors:

1. The potential volume of the char material was calculated at sixty tons per day.(2)
2. The composition the char did not vary by more than 0.5% in ratio of items.

These two considerations prompted further study and application evaluations.

Materials and Methods

One ton of shredded used automobile tires were processed using the Svedala Pyrolysis System (3), The shreds were reduced to a gas, "oil" and char. The char fraction is one third of the feed weight ,six hundred sixty seven pounds yield per ton of tires. Of the six hundred and sixty seven pounds of char, eighty five percent is carbon black and fifteen percent is ash. The char was ground to a uniform mesh size (4) to allow blending and dispersion to occur more easily in subseqnent formulations. The char was used in the following applications in order to determine the value added.

Results

Simultaneous Mercury, Sulfur Dioxide and Nitrous Oxide control in coal combustion by adsorption. The tire derived char was compared to silver impregnated activated carbon at laboratory level to ascertain the sorbent performance. Early tests showed that the char derived from pyrolysis of used automobile tires was equal to the silver impregnated activated carbou, indeed Mercury sorption on tire-derived activated carbon was identified as the most promising application.(5).

Carrier media for distillation of wastes derived from ink, paint, coatings and dry cleaning processes. The char derived from the pyrolysis of used automobile tires was evaluated as a "carrier" for mixed wastes generated by the paint, ink and coatings industries. The wastes evaluated contained aliphatic, aromatic solvents dispersed with pigment, filler, plasticizer and resins. Addition of 7.0 to 11.0% of the char created a mixture that allowed complete evolution of the solvents and absorbed the remaining ingredients of the waste creating a dry solid matrix. The dry solid was then re-ground to a uniform size and evaluated as an extending material for adhesives, synthetic lumber.(6)

Char may be used as an extender in adhesives, coatings and cements. Additions of 3.0 to 7.0% of char to blends of vinyl or rubber cements resulted in lower raw material cost with no loss of physical or chemical properties. The modified cements were tested in floor adhesives, tile adhesives and panel-stick compounds. Neither tack nor drying characteristics are affected by the addition. A stiffening of the finished adhesive bond was determined but did not affect the permanence of the bond.(7)

Discussion

Each application outlined above has been evaluated by no less than three investigators. Work done by others, including Advanced Fuel Research, Rohm & Haas, Morton International Automotive Finishes Group and others confirm that the inclusion of tire derived char, when properly ground and classified, can be nsed as a pre-engineered extender and physical property modifier. Extensive aging tests are being conducted on products utilizing the char. Among the properties within new rubber products that are affected include hardness, elongation, tensile and compression set.(8)

Conclusions.

The investigation of pyrolysis systems appears meaningful in light of the various uses found for the char produced through thermal conversion of used automobile tires. The economic model (9) represents an average value of the char at no less than $0.18 per pound. This "value" coupled with the value of the collected oil product and the energy value provides the support for re-evaluating pyrolysis as one technology to diminish the stockpiles of used tires.

Acknowledgements

We are grateful to Advanced Fuel Research and especially thankful for the meaningful assistance of our colleague Dr. Marek Wojtowicz. We would also like to thank Dr. Mark A. Petrich who was instrumental in the early work on tire char characterization. Special assistance was also provided by Marshall J. Field, President of United Carbon Corporation.

References

(1) Dr. Mark A. Petrich, Northwestern University, Chemical Engineering Department, Evanston Illinois.
(2) United Carbon Corporation, planned facility at California City California, Business Plan and conversation with Marshall J. Field, President.
(3) Michael H. Weinecke, Senior Development Engineer, Svedala Industries, Test Center, Oak Creek Wisconsin; Results of On-Going Production of char product.
(4) Ibid. Svedala Grinder Division Equipment
(5) Marek Wojtowicz, Advanced Fuel Research, SBIR Phase I study, East Hartford Connecticut
(6) David Miklos, Environmental Manager, Morton Automotive Group, Rohm & Haas Corporation, Lansing Illinois, Results of testing and production results.
(7) Gary Post, Applied Recycling Technologies Inc. St. Petersburg Florida. Current use of char in composite lumber production.
(8) Steve Mobley, ProTurn Corporation, Oregon City Oregon, Urethane Foam Rubber mechanical parts used in construction equipment.
(9) Economic model available upon request to author.

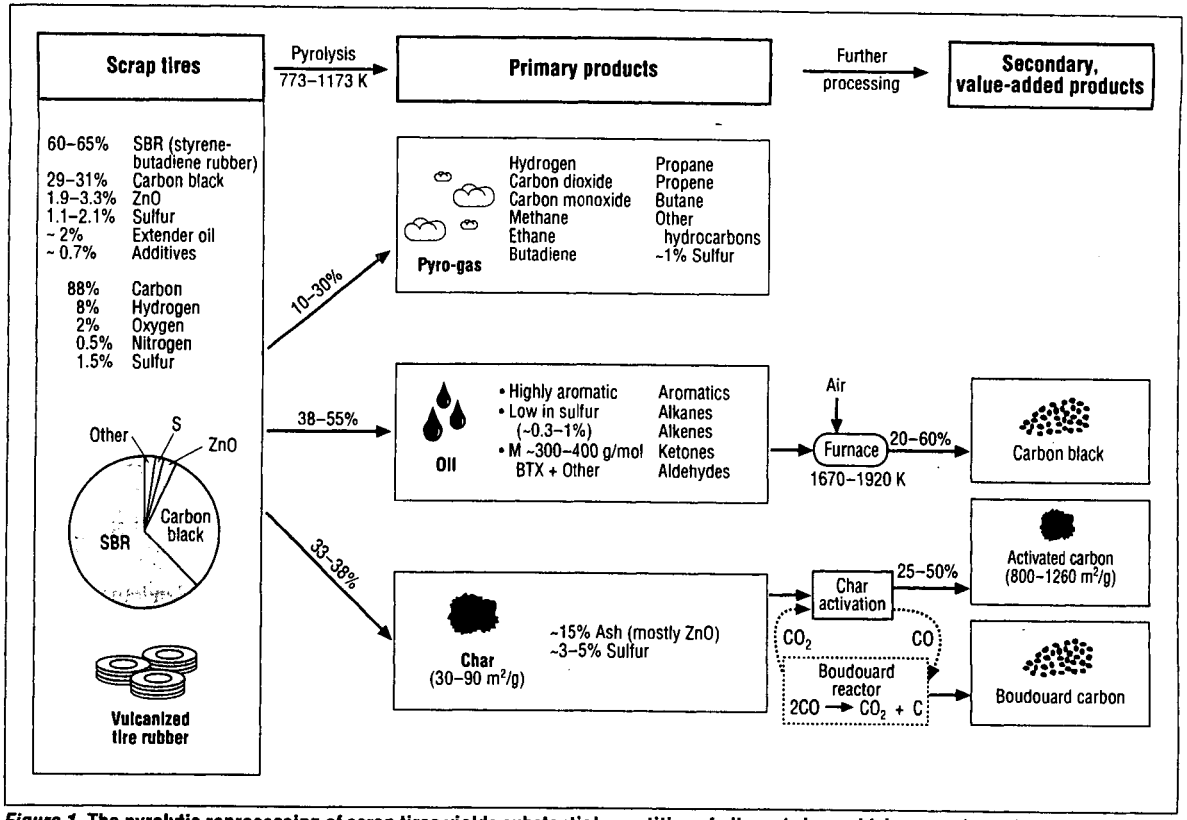

Figure 1. **The pyrolytic reprocessing of scrap tires yields substantial quantities of oils and char, which can undergo further processing to secondary, value-added products.** Char upgrading results in producing high-surface-area activated carbon and Boudouard carbon. Ash-free oils are turned into high-quality carbon black, or the oils can be separated into valuable chemical feedstocks by distillation.

IMPROVED WOMBAT METHOD FOR PROCESSING SCRAP TIRES INTO USEFUL MATERIALS

by
David L. Wertz
Department of Chemistry and Biochemistry, The University of Southern Mississippi,
Hattiesburg, MS 39406
david.wertz@usm.edu
and
Chris D. Deaton
WOMBAT Technologies International, Inc.,
Biloxi, MS 39531
info@omniinstruments.com

Keywords: Scrap tire degradation, economics

The Wertz Oxidative Molecular Bombardment at Ambient Temperature (WOMBAT) process is a sequence of redox reactions which has been used for several years to degrade scrap tires. This process has, to date, been conducted in adiabatic chemical reactors constructed either from poly-vinyl chloride and/or stainless steel. It has the potential to impact the scrap tire inventory in the United States (and elsewhere) which now has reached about three billion and is increasing by 250-300 million annually just in the United States. As previously shown, the WOMBAT process degrades the tire into four recoverable component parts: (a) the steel from its tread and its bead wire sections, (b) the rubber backing(s), (c) the fibers, and (d) a particulate which is dispersed in the reactor fluid. These results are summarized in Figure 1. After washing the steel, the rubber mats, and the fibers, these components may be separated and then used without further treatments. The particulate has typically been removed from the reactor fluid and then collected by centrifugation and/or filtration. After washing the collected particulate with water and drying in a convection oven, the resulting gel is converted to a carbon-based powder by light grinding. The resulting powder has highly irregular particle surfaces and a high, but somewhat variable, oxygen content.

These high carbon particles are effective as sequestering agents for several divalent cations, eg. Ca(II), Cu(II), Pb(II), Hg(II), etc. In addition, the black powder has a heat content ca. 30% higher than the heat content of the typical bituminous coal and a sulfur content in the 0.3 - 1.0% weight percent range even though this powder contains 10-15% oxygen by mass. The economic potential of the black powder recovered from degrading the tire is being explored based on its potential use as a sequestering agent and as a high energy, low ash, low polluting fuel. Both of these potential uses impact the economic model for the WOMBAT process (Figure 2). While the WOMBAT process has achieved its initial goal of degrading the tires into useful end products while generating no hazardous waste, the current reaction procedures have two drawbacks -- the process is quite slow, and the process requires too much reactor fluid (i.e., catalyzed nitric acid).

These limitations have been due, at least in part, to limitations in the design and the operation of our previous reactors. The WOMBAT IV reactor is now available and is being utilized in studies designed to minimize the process problems noted above. In addition, the WOMBAT IV reactor is a significant step forward in a concept of "complete" process

automation.

In an attempt to accelerate the reactor sequences and to improve the requisite fluid/tire materials ratio, several new reactor parameters have been introduced into our process procedures. To date, the effect(s) of controlling and increasing temperature, adding compressed air, and improving the fluid circulation within the reactor have all been studied using our new WOMBAT IV reactor (see Figure 3). In addition, the degradation of the reactor fluid is being studied in an attempt to develop a sensor which will allow for control of the entire process by microprocessor(s).

CONCLUSION. The rate(s) of at least some of the key reactions involved in the WOMBAT process have been accelerated by one order of magnitude.

ACKNOWLEDGMENT. The sponsorship of the United States Department of Agriculture (Small Business Innovative Research Phase I grant), the Mississippi Department of Environmental Quality, two phase 0 SBIR grants from the State of Mississippi, and The University of Southern Mississippi is gratefully appreciated.

SCHEMATIC OF THE WOMBAT PROCESS

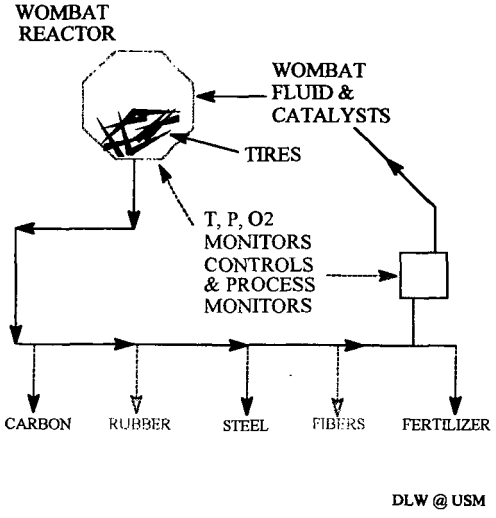

Figure 1

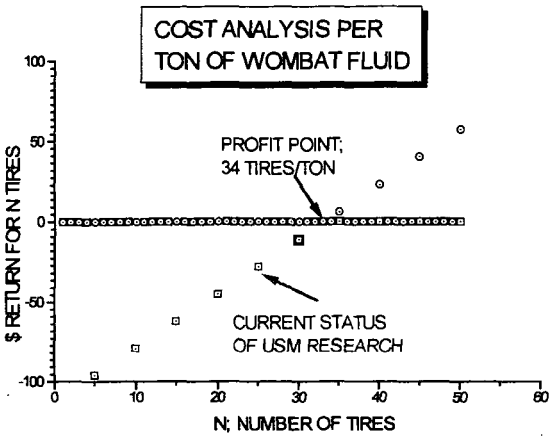

Figure 2

SCHEMATIC OF WOMBAT REACTOR

FLOW OF WOMBAT FLUID

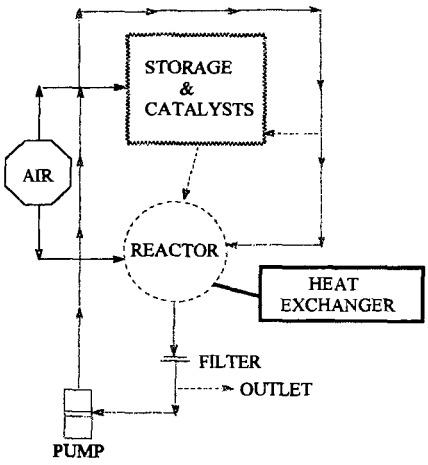

DLW@ USM

Figure 3

The Nature of Porosity in Carbons Derived from Scrap Automobile Tires

Eric M. Suuberg and Indrek Aarna
Division of Engineering, Brown University
Providence, RI 02912 USA
Tel. (401) 863-1420, E-mail *Eric_Suuberg@Brown.edu*

Keywords: activated carbon, porosity, surface area

Introduction

The use of scrap automotive tires for the production of activated carbons has been proposed by many investigators [e.g., 1-4]. The conversion of a problematic waste product to a potentially valuable industrial material has been the basis of possible commercial interest. It is, however, very clear that the ability to produce a material which is a legitimate replacement for currently utilized activated carbons is a prerequisite for moving towards actual commercialization. One of the key criteria for evaluating the potential of these materials concerns the nature of the porosity developed during their activation. This paper presents some detailed evaluations of the porosity developed under certain activation procedures. The research was not specifically aimed at identifying practical processing conditions, but instead sought to provide general insights concerning the development of porosity in this class of materials.

Experimental

The char used in this work was prepared from shredded tire crumb provided by Advanced Fuel Research (AFR) of East Hartford, Connecticut. The original tire particle diameter was about 1 cm, and its ash content was approximately 5%. All samples were initially pyrolyzed in a tube furnace at 973 K for five minutes, in a flow of high purity nitrogen. The yields of char ranged from 35 to 40% and averaged 36%. This is typical of yields from such tire pyrolysis experiments and is in excellent agreement with the results obtained by Teng et al. for the same material pyrolyzed at the same temperature [4]. Following pyrolysis, the char was ground to a powder in a mortar and sieved to a particle size between 320-420 μm. For the activation experiments reported here, the char was further pyrolyzed under nitrogen for one hour at 1173 K prior to activation. Following this second period of pyrolysis, the ash content of the char averaged 15% by mass.

Adsorption isotherms were determined in an automated volumetric gas adsorption apparatus (Autosorb 1, Quantachrome Co.). Adsorption of N_2 was performed at 77 K and adsorption of CO_2 at 195 K. Before measurements, samples were outgassed at 573 K for at least four hours in vacuum. Many were outgassed at 673 K for even longer times. This had no apparent effect on the results.

Char reactivity measurements and activation were performed in an Online Instruments TG-plus thermogravimetric analyzer. The reactions were performed in a mixture of helium and reactant gas (O_2, NO or CO_2), flowing at a rate of about 220 cm^3/min. Samples of 30-50 mg were dispersed on a circular platinum pan with a large flat surface and raised sides, resulting in a particle beds of about 1 mm thickness. Temperatures between 773-973 K were used for gasification with NO and CO_2, and temperatures between 573-748 K for O_2. The variation in temperature had no effect on the development of porosity. The partial pressures of oxidizing gases were 0.82, 2.02 and 4.80 kPa for NO, O_2 and CO_2, respectively. Char samples were outgassed at 1173 K for 30 minutes prior to reactivity measurements or activation. Burnoff is expressed on a dry-ash free basis.

Results and Discussion

The freshly pyrolyzed tire char is not a suitable for most activated carbon applications, due to its very low surface area. The materials that we produced had BET surface areas in the range from 54 to 87 m^2/g, which is typical of such unactivated materials. Thus it was clear that some activation of the material necessary. In the present paper, only the results of physical activation in oxygen, carbon dioxide and nitric oxide are presented.

The nitrogen isotherms on the unactivated material are unremarkable. A typical isotherm is shown on a logarithmic scale in Figure 1. Only very modest microporosity is observed, and there is no hysteresis observed in any portion of the isotherm. Standard Dubinin-Radushkevich (DR)

micropore analysis [5] of these data provides an estimate of micropore volume of 0.027 cc/g. This value was roughly a factor of three greater than the estimate of microporosity from an analysis of carbon dioxide isotherms on the same material. We have interpreted this as evidence for the existence of fairly wide microporosity which can be filled by nitrogen at 77 K, but not by carbon dioxide at 195 K.

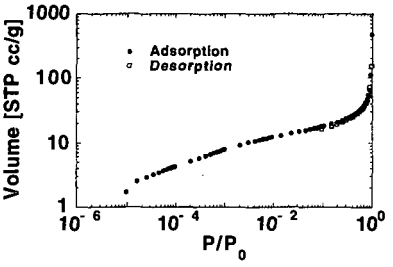

Figure 1. Typical N_2 isotherms on unactivated tire char.

The data of Fig. 1 may also be analyzed to provide an estimate of average pore radius. Assuming for simplicity cylindrical pores, the average radius r may be calculated from:

$$r = 2 * V_{pores} / S$$

where S represents the measured surface area. The values thus obtained for the raw chars range from 170 to 230 Å. It has been earlier noted that the yields of char from tire pyrolysis are generally quite comparable to the content of carbon black in the original tires. This is logical, since the rubber components themselves are quite volatile, and the carbon black can be expected to be nonvolatile. Electron microscopy has shown that our tire chars have a "grape cluster" appearance, consistent with the preservation of non-volatile carbon black particles in the char. In an aggregate solid made up of nearly spherical grains, the size scale of porosity is comparable to the diameter of the grains, i.e., the carbon black particles that constitute the raw tire char. The above average pore radius, thus implies a grain size typical of ASTM group 4 or 5 carbon blacks. These carbon blacks, in the raw state, typically exhibit a (purely external) surface area of around 35 to 70 m^2/g. This is clearly comparable to the values measured for these chars. Thus it may be concluded that the original char particles exhibit porosity determined by the residual carbon black grains. Again, such carbons are of little practical interest as activated carbons.

Upon activation, there is a very large increase in porosity. The adsorption isotherms for the oxygen activated material are shown in Figure 2.

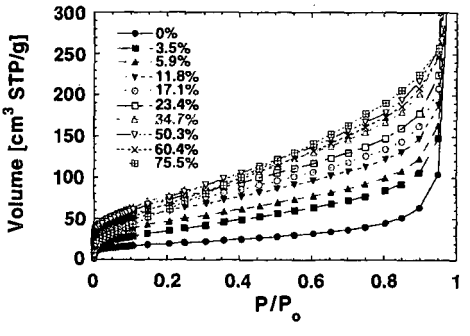

Figure 2. Nitrogen 77 K isotherms for samples activated in 2% oxygen.

It made little difference whether the chars were burned off in 2 % oxygen or in air (21 % oxygen) - the isotherm depended only upon level of burnoff, not the oxygen partial pressure used to achieve it. Likewise, temperature of activation made no difference to the development of porosity with burnoff in a range from 673 K to 773 K (400°C to 500°C). Naturally, both the oxygen partial

pressure and temperature did significantly affect the rates of activation. The similarity of porosity development observed under this wide range of conditions implied that the activating reactions were not taking place in a transport controlled regime, at least on the scale of porosity being developed.

Figure 3 shows the variation of nitrogen DR micropore volume with burnoff. Apart from re-emphasizing that the porosity development was not sensitive to activation conditions in oxygen, these results also indicate an apparent maximum in micropore volume at a burnoff of around 40%. On the other hand, the standard BET analysis [5] of the isotherm data show no significant decline in area with burnoff over 40% (see Figure 4). Generally, the BET surface area is associated with microporosity, so there is an apparent inconsistency between the results of Figures 3 and 4. The apparent contradiction is resolved by a density functional theory [6,7] analysis of the isotherm data. The results of the DFT analysis are shown in Figure 5.

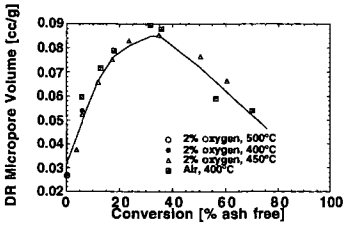

Figure 3. DR analysis of microporosity in tire chars activated in oxygen.

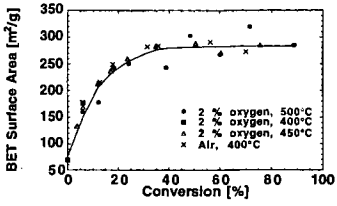

Figure 4. BET surface area of chars activated in oxygen.

The cumulative pore size distribution, on a pore volume basis, is shown in Figure 5. These results were obtained from DFT theory. They show that above 38.8% burnoff, there is a very significant loss of microporosity with burnoff (pores with halfwidths less than 10Å). By 88.7% burnoff, the micropores have virtually disappeared.

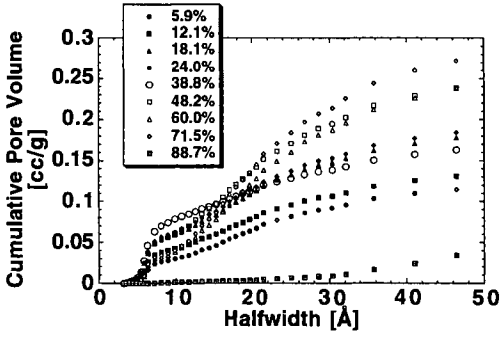

Figure 5. DFT pore size distributions as a function of burnoff in oxygen.

The decrease in micropore volume with burnoff above 38.8% burnoff is consistent with Figure 3. On the other hand, DFT theory can also be used to calculate surface area. The results of the calculation are shown in Figure 6. There is good agreement between the BET areas and those from DFT theory, with one notable exception (the sample at highest burnoff). Leaving this one exception aside, it is clear that the reason for the apparent discrepancy between the trends in micropore volume and BET area is that there is actually a significant contribution of mesopores to surface area, at high burnoffs. That is, the original assumption that surface area is dominated by micropores is not correct. The exceptional point at 88.7% burnoff exhibited a rather more curved BET plot than did the other samples. Therefore the fact that this point appeared to give the same surface area as the other lower burnoff samples is regarded as merely fortuitous. A similar high burnoff decline in DFT surface area was observed in another series of samples activated in air, so it is believed that the trend suggested by this point is real.

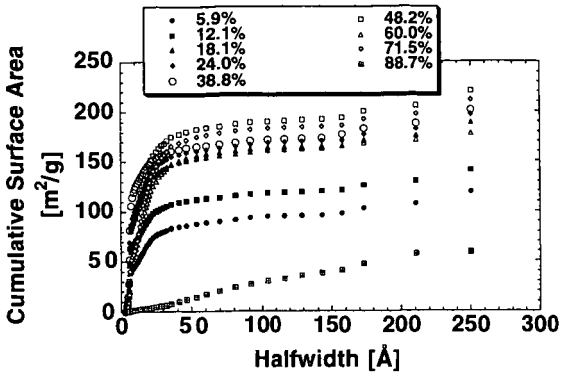

Figure 6. DFT cumulative surface areas for tire chars activated in 2% oxygen.

The development of surface area with activation follows a different pattern in different oxidizing gases. The results are shown in Figure 7. In this case, an attempt was made to match the initial gasification rates as closely as possible, so as to avoid differences in any possible role of mass transport. The oxygen activated samples appear to follow a different course than do the CO_2 and NO activated samples; the latter two gases appear much more effective in opening up surface area.

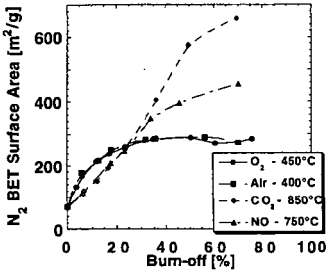

Figure 7. The development of BET surface area in oxygen, CO_2 and NO.

The ability of CO_2 to develop microporosity is explored in more detail, using DFT methods, in Figure 8. It is apparent that the difference between CO_2 and O_2 activation has to do with the absence of micropore-destroying processes at higher burnoffs. The CO_2 activation processes continue to develop micropores up to much higher burnoffs. This is reflected in the higher BET surface areas observed at high burnoffs.

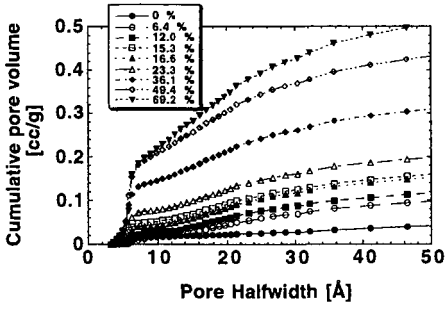

Figure 8. The development of porosity in CO_2 activation, examined using DFT.

It is interesting to compare the development of porosity in oxygen and carbon dioxide at lower

burnoffs. This is done, again using DFT methods, in Figure 9.

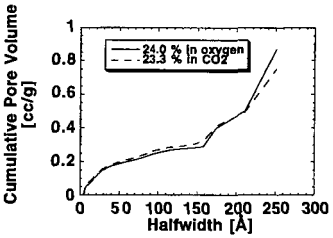

Figure 9. A comparison of porosity development during oxygen and carbon dioxide activation, at low burnoffs.

Figure 9 shows remarkable agreement in the pore size distributions obtained at already significant extents of burnoff. This would not have been anticipated, based upon the very different high burnoff behaviors of the samples activated in these two gases. The results with NO are also virtually identical in this range of burnoff (not shown here). It is as though up to a certain burnoff, the activation processes are being forced to follow a very similar pathway, but beyond that point, the differences in the nature of the reacting processes begin to manifest themselves. It may be that there is a certain fraction of carbon that is very much more reactive than the remaining carbon, and is removed first. This carbon would have to be associated with the carbon black particles, for the reasons noted above. It should be however noted that the accompanying reactivity studies gave no evidence of an abrupt change in carbon reactivity at burnoffs between 30 and 40% in either oxygen or carbon dioxide. Thus what drives the preferential removal of certain carbon atoms over others must be associated with subtle differences in reactivity. We have examined the possible role of catalysis in determining this behavior [8]. It is clear that the gasification is catalyzed by the inorganic impurities in the original tire material, but that this does not particularly influence the behavior of interest here. The catalysts appear to drive the formation of somewhat larger porosity in these samples.

Consequently, it appears as though the tire chars have an inherent propensity to form a certain amount of micro- and small mesoporosity. This tendency must be associated with the original carbon black particles in the tire, but it is not clear from the present work whether this tendency can be influenced by pyrolysis conditions. Beyond a certain burnoff, different oxidizing gases promote different types of porosity development, and can heavily influence the product carbon characteristics.

Acknowledgment

The support of the National Science Foundation under grant BES-9523794 and the US DOE under grant DE-FG22699-FT40582 are gratefully acknowledged.The encouragement and assistance of various personnel at Advanced Fuel Research, particularly Drs. Michael Serio and Marek Wójtowicz, is also gratefully acknowledged. Thanks are also due to Dr. Anil Prabhu of Quantachrome Corporation, for kindly allowing us to utilize a pre-release version of their DFT software.

References

1. Williams, P.T., Besler, S., Taylor, D.T., Fuel, 69, 1474 (1990).
2. Merchant, A. A., Petrich, M., AIChEJ, 39, 1370 (1993).
3. Ogasawara, S., Kuroda, M., Wakao, N., I&EC Res., 26, 2552 (1987).
4. Teng, H., Serio, M., Wojtowicz, M., Bassilakis, R., Solomon, P., I&EC Res., 34, 3102 (1995).
5. Gregg, S., Sing, K., *Adsorption, Surface area and Porosity*, Academic Press, 1982.
6. Evans, R., Marconi, U.M.B. and Tarazona, P. *J. Chem. Soc. Faraday Trans. II 82*, 1763 (1986).
7. Lastoskie, C., Gubbins, K.E. and Quirke, N. *J. Phys. Chem., 97*, 4786 (1993).
8. Suuberg, E.M. and Aarna, I., paper prepared for the *3rd Joint China/USA Chemical Engineering Conference,*, Beijing, September, 2000.

PYROLYSIS PROCESSING OF MIXED SOLID WASTE STREAMS

Michael A. Serio, Yonggang Chen, and Marek A. Wójtowicz

Advanced Fuel Research, Inc., 87 Church Street, East Hartford, CT 06108, USA

Eric M. Suuberg

Division of Engineering, Brown University, Providence, RI 02912 USA

KEYWORDS: Solid Waste, Pyrolysis, Life Support

ABSTRACT

The NASA objective of expanding the human experience into the far reaches of space will require the development of regenerable life support systems. A key element of these systems is a means for solid waste resource recovery. The objective of this work was to examine the feasibility of pyrolysis processing as a method for the conversion of solid waste materials in a Controlled Ecological Life Support System (CELSS). A composite mixture was made consisting of 10% polyethylene, 15% urea, 25% cellulose, 25% wheat straw, 20% Gerepon TC-42 (space soap) and 5% methionine. Pyrolysis of the composite mixture produced light gases as the main products (CH_4, H_2, CO_2, CO, H_2O, NH_3) and a reactive carbon-rich char as the main byproduct. Significant amounts of liquid products were formed under less severe pyrolysis conditions, but these were cracked almost completely to gases as the temperature was raised. A primary pyrolysis model was developed for the composite mixture based on an existing model for whole biomass materials.

INTRODUCTION

A key element of a CELSS is a means for solid waste resource recovery. Solid wastes will include inedible plant biomass (IPB), paper, plastic, cardboard, waste water concentrates, urine concentrates, feces, etc. It would be desirable to recover usable constituents such as CO_2, H_2O, hydrogen, nitrogen, nitrogen compounds, and solid inorganics. Any unusable byproducts should be chemically and biologically stable and require minimal amounts of storage volume. Many different processes have been considered for dealing with these wastes: incineration, aerobic and anaerobic biodigestion, wet oxidation, supercritical water oxidation, steam reforming, electrochemical oxidation and catalytic oxidation [1-13]. However, some of these approaches have disadvantages which have prevented their adoption. For example, incineration utilizes a valuable resource, oxygen, and produces undesirable byproducts such as oxides of sulfur and nitrogen. Incineration also will immediately convert all of the waste carbon to CO_2, which will require storing excess CO_2.

"Pyrolysis," in the context of this paper, is defined as thermal decomposition in an oxygen free environment. Primary pyrolysis reactions are those which occur in the initial stages of thermal decomposition, while secondary pyrolysis reactions are those which occur upon further heat treatment. A pyrolysis based process has several advantages when compared to other possible approaches for solid waste resource recovery: 1) it can be used for all types of solid products and can be easily adapted to changes in feedstock composition; 2) the technology is relatively simple and can be made compact and lightweight and thus is amenable to spacecraft operations; 3) it can be conducted as a batch, low pressure process, with minimal requirements for feedstock preprocessing; 4) it can produce several usable products from solid waste streams (e.g., CO_2,CO, H_2O, H_2, NH_3, CH_4, etc.); 5) the technology can be designed to produce minimal amounts of unusable byproducts; 6) it can produce potentially valuable chemicals and chemical feedstocks; (e.g., monomers, hydrocarbons, nitrogen rich compounds for fertilizers) 7) pyrolysis will significantly reduce the storage volume of the waste materials while important elements such as carbon and nitrogen can be efficiently stored in the form of pyrolysis char and later recovered by gasification or incineration when needed. In addition to being used as the primary waste treatment method, pyrolysis can also be used as a pretreatment for more conventional techniques, such as incineration or gasification. A summary of the pyrolysis processing concept is shown in Figure 1.

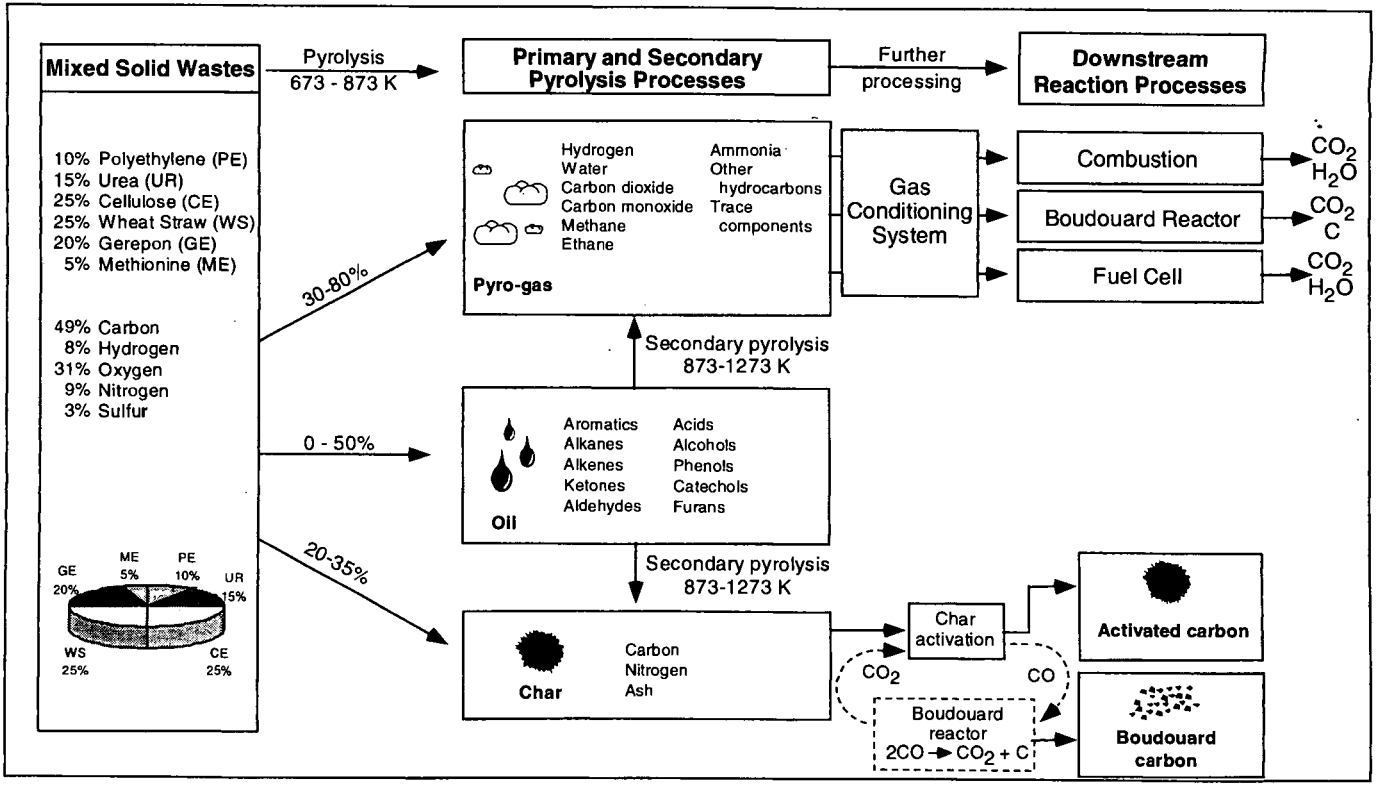

Figure 1. Summary of proposed pyrolysis-based solid waste processing scheme.

The primary disadvantages of pyrolysis processing are: 1) the product stream is more complex than for many of the alternative treatments; 2) the product gases cannot be vented directly in the cabin without further treatment because of the high CO concentrations. The former issue is a feature of pyrolysis processing (and also a potential benefit, as discussed above). The latter issue can be addressed by utilization of a water gas shift reactor or by introducing the product gases into an incinerator or high temperature fuel cell.

EXPERIMENTAL METHODS

Sample Selection - It was decided to use a model waste feedstock similar to what was used in a previous study at Hamilton Standard [11], the so-called "Referee mix." That study used 10 wt. % polyethylene, 15% urea, 25% Avicel PH-200 cellulose, 25% wheat straw, 10% Gerepon TC-42 (space soap) and 5% methionine. The materials that were obtained and the elemental compositions of each (on a DAF basis) are given in Table 1. A different sample of Avicel cellulose was used (PH-102), as a supply was already on hand and significant amounts of data had been generated with this material for a private client in a previous study. It was thought that the difference between these two cellulose samples would be small and that there was an advantage to using a material whose individual pyrolysis behavior had already been characterized. The NIST wheat straw sample was previously studied under a USDA project [14]. The Gerepon TC-42 is the same as the Igepon TC-42, but the name was changed since the product line was sold to a new company (Rhône-Poulenc). It is a soap which is made from coconut oil, so its exact formula is unknown. The composition was estimated by assuming that most of the fatty acids were C_{12}. The technical name for Gerepon TC-42 is sodium methyl cocoyl taurate.

TG-FTIR System - The samples in Table 1 were obtained and subjected to thermogravimetric analysis with FT-IR analysis of evolved gases (TG-FTIR) at 10 °C/min and 30 °C/min. Details of the TG-FTIR method can be found in references [15] and [16]. The apparatus consists of a sample suspended from a balance in a gas stream within a furnace. As the sample is heated, the evolving volatile products are carried out of the furnace directly into a 5 cm diameter gas cell (heated to 150 °C) for analysis by FT-IR. In the standard analysis procedure, a ~35 mg sample is taken on a 30 °C/min temperature excursion in helium, first to 150 °C to dry, then to 900 °C for pyrolysis. After cooling, a small flow of O_2 is added to the furnace and the temperature is ramped to 700 °C (or higher) for oxidation in order to measure the amount of inorganic residue. The TG-FTIR system can also be operated with a post pyrolysis attachment to examine secondary pyrolysis of the volatile species (see below).

During these excursions, infrared spectra are obtained approximately once every forty-one seconds. The spectra show absorption bands for infrared active gases, such as CO, CO_2, CH_4, H_2O, C_2H_4, HCl, NH_3, and HCN. The spectra above 300 °C also show aliphatic, aromatic, hydroxyl, carbonyl and ether bands from tar (heavy liquid products). The evolution rates of gases derived from the IR absorbance spectra are obtained by a quantitative analysis program. The aliphatic region is used for the tar evolution peak. Quantitative analysis of tar is performed with the aid of the weight-loss data in the primary pyrolysis experiments.

The TG-FTIR method provides a detailed characterization of the gas and liquid compositions and kinetic evolution rates from pyrolysis of materials under a standard condition. While the heating rates are slower (3-100 °C/min) than what is used in many practical processes, it is a useful way of benchmarking materials and was used in this study for characterizing both the primary and secondary pyrolysis behavior of the model waste samples and the individual components. In addition, Advanced Fuel Research, Inc. (AFR) has developed kinetic models based primarily on TG-FTIR data which can be extrapolated over a wide range of conditions.

Differential Scanning Calorimetry (DSC) - Measurements of the thermodynamics of the pyrolysis process, were made using differential scanning calorimetry (DSC) at Brown University. Samples of each of the materials in Table 1 were sent to Brown. The DSC experiments were done by heating at 10, 30 and 60 °C/min. These heating rates were the same or similar to the heating rates used in the TG-FTIR experiments, so a direct comparison could be made. A TA Instruments 2910 DSC system, with a maximum operating temperature of 600 °C, was employed in the DSC work. The sample cell was operated under a nitrogen flow rate of 100 cm^3/min in order to keep the cell free of oxygen during the measurements. In preliminary work,

this was noted to be important. Small amounts of oxygen, participating in a combustion reaction, can significantly influence the thermal characteristics of the process.

Table 1. Elemental Analysis of Individual and Composite Samples (DAF wt.%)

Sample	C	H	O	S	N
Polyethylene[a] (Aldrich)	85.7	14.3	0.0	0.0	0.0
Cellulose[b] (Avicel PH-102)	44.0	6.2	49.8	~0.0	~0.0
Wheat Straw[b] (NIST)	48.0	6.2	44.9	0.2	0.7
Urea[a] (Aldrich)	20.0	6.7	26.6	0.0	46.7
Gerepon[c] TC-42 (Rhône -Poulenc)	60.5	11.5	11.5	11.5	5.0
Methionine[a] (Aldrich)	40.3	7.4	21.4	21.5	9.4
Composite	48.7	8.2	31.0	3.4	8.7

Notes: DAF = Dry, Ash Free
a = determined from chemical formula
b = determined by Huffman Laboratories (Golden, CO)
c = estimated from approximate chemical formula

Aluminum sample pans were used for the DSC experiments in a partially sealed mode. This was done by pushing down the top sample pan cover gently onto the bottom pan containing the sample. Following this, three small pinholes were poked into the sample pan to allow a limited amount of mass loss from the pan. This configuration has been used previously in work on cellulose samples [17], and gives results which are consistent with pyrolysis in a confined system with a slow rate of mass bleed out of the system. It was felt that this would be reasonably representative of a pyrolysis processing system. Typically, about 10 mg of sample was used in an experiment.

In many cases, particularly with charring samples, the initial DSC run was followed by a cooling of the sample back down to room temperature, followed by a retrace of the original heating profile. This procedure provided a background trace attributable to the heat capacity of the char residue. In cases involving formation of a char residue, the mass loss of the sample during the first heating was also established. These values were compared with the TG-FTIR results, to verify whether the pyrolysis was occurring in a consistent manner, or in a different manner due to the increased mass transport resistance in the DSC pans.

RESULTS AND DISCUSSIONS

TG-FTIR Results for Primary Pyrolysis - An example of some representative data is shown in Table 2, which includes the average results of all the runs done at heating rates of 30°C/min. Similar results were obtained at 10°C/min [18,19]. For all of the samples, data from primary pyrolysis experiments for the same nominal pyrolysis conditions for each sample are generally in good agreement. For example, in the case of cellulose, there are differences in CO_2 yields that can probably be attributed to small air leaks in the system. For polyethylene, the material experiences a rapid and essentially complete depolymerization to tar which drives the balance pan below zero weight. Since the tar yields are ultimately determined by difference, this phenomenon results in integration errors which lead to tar yields above 100%. For the minor (trace) species for all of the samples, integration errors are also a concern and the results which are thought to be influenced mainly by noise are indicated by italics in Table 2.

For each of the samples, the data include moisture, total volatiles, fixed carbon, and ash. The yields of tar, CH_4, water, CO_2, and CO are reported as major pyrolysis products. In most cases, the minor pyrolysis products which are quantified include SO_2, C_2H_4, CS_2, NH_3, COS, and olefins and the amounts of these latter product are usually barely above the noise level. Hydrogen is not reported since the gas is not IR active. However only small amounts of

hydrogen are formed in primary pyrolysis experiments (<1 wt.%). It can be an important product from secondary pyrolysis experiments and for these experiments, the FT-IR measurements were supplemented by GC (see below).

The selection of the minor species to report is somewhat arbitrary and the current set of gases is historically based on our extensive work on coal pyrolysis. For some of the samples, (urea, methionine, composite), the selection of species was changed in order to reflect the important major and minor pyrolysis products. Obviously, any gas can be quantified that is IR active and for which a calibration exists. In the case of the cellulose, wheat straw and Gerepon TC-42, the results could be made quantitative without any new calibrations since the major products were in our existing reference library. However, for the urea, methionine, and composite mixture, some additional calibrations had to be done in order to describe the evolution of some of the important products.

Table 2 - Average Results from Primary Pyrolysis Experiments in TG-FTIR System at 30°C/min (wt.%, As-Received Basis)

Sample	Cellulose	Wheat Straw	Polyethy-lene	Urea	Gerepon TC-42	Methion-ine	Composite Mix
Moisture	3.5	5.2	0.6	1.8	67.1	0.0	0.6
Volatiles	94.4	69.4	99.2	98.2	27.2	99.2	87.0
Fixed Carbon	1.3	17.5	0.0	0.0	2.0	0.0	12.4
Ash	0.5	7.8	0.0	0.0	4.8	0.8	0.0
Tars	91.2	30.0	101.4+	0.00	20.8	46.55	30. 9
CH_4	0.23	0.88	0.11	0.00	0.13	0.00	0.56
C_2H_4	0.04	0.32	0.0	4.54	*0.14*	0.00	0.40
H_2O	7.81	22.74	1.30	21.94	3.12	3.74	23.30
CO_2	2.72	10.50	0.54	1.83	2.42	6.96	9.80
CO	1.04	6.56	0.00	1.66	0.85	0.00	5.58
NH_3	*0.05*	*0.07*	0.00	13.89	*0.26*	0.58	0.86
COS	0.00	*0.00*	0.00	0.00	*0.13*	0.00	0.60
SO_2	0.00	0.24	0.00	0.00	0.3	0.06	1.10
Cyanic acid (CHNO)				22.43			0.40
Cyanuric acid ($C_3H_3N_3O_3$)				0.56			
Biuret				32.70			
Methionine						27.77	
Methylthiopropyl amine						13.05	11.87

Notes: Yields are given on an as-received wt.% basis; numbers in italics are influenced by noise and may not be reliable; + indicates numbers that are influenced by balance errors due to very rapid devolatilization; all runs done at standard carrier gas flow rate of ~400 cm^3/min helium.

Both the cellulose and the polyethylene undergo nearly complete devolatilization to 100% tar plus gas. As expected, the cellulose and wheat straw produce oxygenated gases in addition to tar. However, the wheat straw produces about 20-25 wt.% char (fixed carbon plus ash) on an as-received basis. The formation of fixed carbon from whole biomass is known to result primarily from the aromatic lignin component of the plant, which typically comprises 20-25% by weight, with the remainder being primarily cellulose and hemicellulose [20]. Previous work at AFR and elsewhere has shown that the weight loss from pyrolysis for whole biomass samples can be understood as a linear superposition of these three main components to a first approximation [14]. However, one can not predict the yields of individual gas species using this approach, probably due to the catalytic effects of the trace minerals present in whole biomass.

Aside from NH_3 and small amounts of H_2O, the pyrolysis products from urea (N_2H_4CO) include cyanic acid, CHNO, and another compound that is probably biuret, $NH_2CONHCONH_2$. The latter two products were initially identified by a target factor analysis program that separates real component spectra from FTIR data. The cyanic acid was verified by pyrolyzing cyanuric acid

($C_3H_3N_3O_3$) a ring compound made essentially of three cyanic acid groups. Cyanuric acid produces cyanic acid and some cyanuric acid (either by evaporation or recombination of the cyanic acid) during pyrolysis. Biuret was tentatively identified by absorption peak positions, and comparison to solid phase spectra in the Aldrich Spectal Library book. The formation path for biuret is most likely from combination of cyanic acid with urea. All the products start evolving at fairly low temperatures, 125 to 145 °C but do not finish until around 420 °C.

Most of the mass loss from Gerepon TC-42 is from drying, due to the large moisture content. Additional water, along with CO_2, tars and small amounts of CO are produced from pyrolysis of the organic part of the soap.

Methionine ($C_5H_{11}O_2N_S$) pyrolysis proceeds in a much simpler fashion than in the case of urea. There is one basic weight loss event centered around 300 °C, producing mostly CO_2 and 3-(methylthio) propylamine. This is probably from decarboxylation of the methionine. To identify which other bonds in the methionine might be breaking, absorption spectra from the TG-FTIR runs were checked for some simple molecules that might result. For example, if the end C-S bond were to break, CH_4 would result. None was found, however. Similarly, there was no C_2H_4, NO, N_2O, NO_2, CH_3SH, CH_3SCH_3, SO_2, or CO and very little NH_3, indicating that the C-S bonds remained intact as did the bonds between the alpha and beta C. The only other thing that happened was a little bit of deamination and some dehydrolysis (as evidenced by water loss) which may have led to a polymerized high molecular weight product (tar). A compound, not yet identified, evolves around 220 to 270°C and accounts for about 25% of the methionine's weight loss. The material does not coincide with any release of other small gases. This means the product is either from direct evaporation of the methionine or some rearrangement is taking place. The hydrogen bonding in the methionine keeps the melting point high (and therefore the vapor pressure low) at around 275°C. Rearrangement could alter the hydrogen bonding and lead to a more easily evaporated material. The remainder of the sulfur mass must be distributed between the tar and this early pyrolyzate.

For the composite mixture, most of these unknown products are inconsequential, because of the relatively small contribution of urea and methionine to the overall product distribution and the product transformations that occur in the mixture due to chemical interactions and catalytic effects. Consequently, it was decided to limit the amount of effort devoted to identification of the products of pyrolysis of pure urea and methionine.

The results for TG-FTIR runs with the composite ("referee") mixture are also shown in Table 2. It can be seen that, in terms of product distribution (char, tar, gas), the results are much more similar to the NIST Wheat Straw sample than the cellulose, polyethylene, Gerepon, methionine, or urea samples. This result makes sense in that the wheat straw is also a composite mixture which consists of cellulose, hemi-cellulose, and lignin, while the composite mixture is made up of 25% cellulose and 25% wheat straw as the largest components. The wheat straw sample also has an elemental composition which is relatively close to that of the composite mixture (see Table 1). Therefore, one might expect similar pyrolysis behavior.

DSC EXPERIMENTS

The general conclusion which can be drawn from these measurements is that the composite mixture pyrolysis is only mildly endothermic (of order 100 J/g), under conditions in which a significant amount of mass loss is permitted to occur during pyrolysis. Confining pyrolysis more completely might be expected to drive the process in an even more exothermic direction, as it does in the case of pure cellulose [17]. In any event, it may be noted that, in comparison to this relatively modest enthalpy of pyrolysis, the sensible enthalpy for heating the sample is quite a bit larger. For example, using a "typical" average heat capacity for cellulose of 2 J/g-K to represent the composite mixture, it can be determined that heating from room temperature to 600°C will itself require 1150 J/g of sample. Additionally, the heat required to evaporate any residual moisture content could also far outweigh this small pyrolysis thermal demand. Thus it may be concluded that the heat of pyrolysis will not be of significant design concern unless conditions far removed from these are to be explored. Most of the heat input required will be to overcome heat losses from the reactor.

RESULTS OF CHAR CHARACTERIZATION STUDIES

Much of the work on char characterization was also done at Brown University. The work at Brown included characterization of the gasification reactivity of the char using a TGA system and pore structure measurements using the Autosorb instrument made by Quantachrome. Char forming experiments were performed under conditions comparable to those at AFR. In addition, samples of char generated at AFR were supplied to Brown.

At both AFR and Brown, reactivity measurements were made using indices known as $T_{critical}$ and T_{late}. These measure the temperature at which a char heated at 30 °C/min in air achieves a reaction rate of 6.5% per min in the early stage of reaction and where it returns to that value in the later stages. Low values of $T_{critical}$ and T_{late} indicate a reactive material and vice versa. The results indicated that these chars are very reactive and would be easy to gasify or combust in order to recover additional carbon and nitrogen. The same conclusions were reached in the more extensive char characterization studies that were done at Brown, which also included characterization of pore structure [18].

TG-FTIR EXPERIMENTS WITH THE POST PYROLYZER (TG-FTIR/PP)

The TG-FTIR system, was used as discussed above, to characterize the primary pyrolysis behavior of the individual components and the composite sample. Under this study, the system was also equipped with a post-pyrolysis system (isothermal secondary pyrolysis unit) in order to study the cracking of the heavy liquids (tars) and other volatiles that are formed during pyrolysis of these materials. This post pyrolysis unit can be operated from 500-1000 °C with an average volatile residence time of 0.4-2.6 seconds at atmospheric pressure. Under the right pyrolysis conditions, the liquids are cracked to produce primarily CO, CO_2, CH_4, H_2, H_2O, and small amounts of carbon.

In the current study, experiments were done with the TG-FTIR/PP system over the temperature range from 600 – 1000 °C in the post pyrolyzer. The helium gas flow rate through the 14 cm^3 volume post pyrolyzer for the "fast" runs was ~400 cm^3/min (at standard conditions). Additional runs were done at lower flow rates (~100 cm^3/min) in order to test the effect of this variable and also to provide gas concentration levels that would allow for simultaneous measurements by FT-IR and GC. Over a temperature range of 600 – 1000 °C, these gas flow rates correspond to a range of residence times for the fast flow conditions of 0.4 to 0.6 seconds and 1.8 to 2.6 seconds for the slower flow conditions, i.e., the flow rates were not adjusted to equalize the residence times at each temperature.

The TG-FTIR/PP experiments were done for both the composite mixture sample and the wheat straw sample. A set of results for the composite mixture, shown in Figure 2, demonstrate the

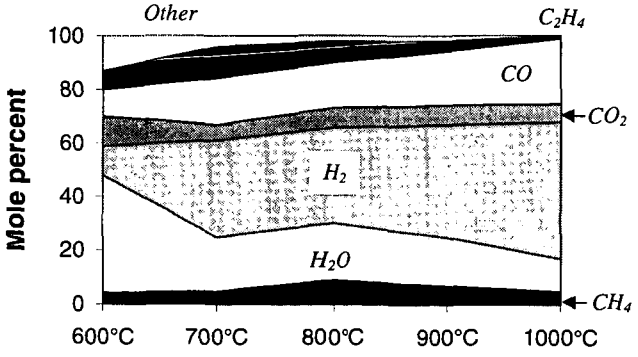

Figure 2. Estimated gas phase composition (mole %, excluding helium carrier) from TG-FT-IR pyrolysis experiments at 30°C/min with the composite mixture followed by secondary pyrolysis over a range of isothermal temperatures.

very strong effect of the post pyrolysis temperature on the product composition. As the post pyrolysis temperature increases, the tar yields decline to zero and the CO yields increase dramatically. The CH_4, H_2O and CO_2 yields go through a maximum. Similar results are observed for post-pyrolysis runs done with the pure wheat straw sample [18]. In order to get yield data on H_2, the GC system was used to take periodic samples.

The data shows that with increasing pyrolysis temperature, the gas composition becomes rich in H_2 and CO and that CH_4, CO_2 and H_2O are also key components. While tars and minor heterotomic species are present at low temperatures, these are largely eliminated as the temperature increases.

These results underscore the significant effect of primary and secondary pyrolysis conditions on the final product mix. There are many variables that can be manipulated for pyrolysis that can be used to compensate for changes in the feedstock composition and/or the desired product yields (e.g., time-temperature history, pressure). This provides a much greater degree of control over the solid waste processing step than is possible for either gasification or incineration. Changing the pyrolysis conditions allows one to effect significant changes in the pyrolysis product distribution (char, tar, gas) and the gas composition. Liquids can be produced if desired (under mild conditions) or cracked to form carbon oxides and fuel gases under severe conditions, depending on what is required for the life support system.

SUMMARY AND CONCLUSIONS

This project demonstrated that it is possible to pyrolyze a representative composite mixture of mixed solid waste materials and produce usable gases as the main products (CH_4, H_2, CO_2, CO, H_2O, NH_3) and a reactive carbon-rich char as the main byproduct. Significant amounts of liquid products were formed under less severe pyrolysis conditions, but these were cracked almost completely to gases as the secondary pyrolysis temperature was raised. A primary pyrolysis model was developed for the composite mixture based on an existing model for whole biomass materials, while an ANN model was used successfully to model the changes in gas composition with pyrolysis conditions [18].

This work has demonstrated that pyrolysis processing meets the requirements of solid waste resource recovery in space, i.e., it produces usable byproducts, with minimal side products, can be tailored to meet changes in the feedstock composition and the product requirements, significantly reduces storage volume, requires low maintenance can be conducted as a batch, low pressure process, and is compatible with the utilities that are present on board a spacecraft (electricity and small amounts of O_2 and H_2O). It should be noted that the pyrolysis gases will require further treatment, such as water gas shift conversion to remove CO, before they can be vented into the cabin. However, these gases could also be introduced into an incinerator or a high temperature fuel cell system with minimal pretreatment.

In future work, a prototype waste pyrolysis system will be developed in collaboration with NASA, Hamilton Sunstrand Space Systems International and Brown University and delivered to NASA. This pyrolyzer will be useful to NASA in at least four respects: 1) it can be used as a pretreatment for an incineration process; 2) it can be used as a more efficient means of utilizing oxygen and recycling carbon and nitrogen; 3) it can be used to supply fuel gases to fuel cells for power generation; 4) it can be used as the basis for the production of chemicals and materials in space.

ACKNOWLEDGEMENTS

The support of this work by the NASA-Ames Research Center under contracts NAS2-99001 and NAS2-00007 is gratefully acknowledged. The COTR was John Fisher and we are very grateful for his support and technical guidance. The authors also wish to acknowledge the contributions of David Marran, Rosemary Bassilakis, and Miriam Leffler of AFR to the experimental work and Robert Carangelo, an independent consultant to the interpretation of the TG-FTIR results. We are also grateful for comments and advice we have received from our colleagues at Hamilton SunStrand Space Systems International, Inc., Joseph Genovese, Philip Birbara, Harold Couch, and Kathy Ferner.

REFERENCES

1 Tri, T.O., Edeen, M.A., and Henninger, D.L., SAE 26th International Conference on Environmental Systems, Monterey, CA, Paper #961592, 8p. July 8-11,1996.

2 Budenheim, D.L. and Wydeven, T., Advances In Space Research (ISSN 0273-1177), Vol. 14, No. 11, P.113-123, Nov. 1994.

3 Flynn, M. and Budenheim, D., Space Technology and Applications International Forum (STAIF-98); Proceedings of The 2nd Conference on Applications of Thermophysics In Microgravity and 3rd Conference on Commercial Development of Space, Albuquerque, NM, P. 835-839, Jan. 25-29, 1998.

4 Ferrall, J.F., Ganapathi, G.B., Rohatgi, N.K., and Seshan, P.K., Technical Report - NASA-TM-109927; NAS 1.15:109927, Jet Propulsion Lab., Pasadena, CA.

5 Bilardo, V.J., Jr. and Theis, R.L.A., Engineering, Construction, and Operations In Space III: Space '92, Vol. 2, P. 1748-1764, May 31-June 4, 1992.

6 Ferrall, J., Rohatgi, N.K., and Seshan, P.K., SAE Paper 921119.

7 Marrero, T.R., NASA/ASEE Summer Faculty Fellowship Research Program Research Reports N86-14078 04-85), 1983.

8 Smernoff, D.T., Wharton, R.A., Jr., and Averner, M.M., Sales Agency and Pricing - HC A99/MF A04, P 263-280.

9 Spurlock, P., Spurlock, J.M., and Evanich, P.L., 21st Conference on Env. Systems, San Francisco, 1991.

10 Roberson, B.J., Lemay, C.S., NASA American Society For Engineering Education (ASEE) Summer Faculty Fellowship Program, Vol. 2, 1993.

11 NASA, Advanced Waste Management Technology Evaluation, Contract NASW - 5005, Final Report, June 1996.

12 Pisharody, S., Borchers, B., Schlick, G., "Solid Waste Processing in a CELSS: Nitrogen Recovery," Life Support & Biosphere Science, 3, pp. 61-65 (1996).

13 Bubenheim, D.L., Wydeven, T., "Approaches to Resource Recovery in Controlled Ecological Life Support Systems," Adv. Space Res., 14 (11), 113-123 (1994).

14 Serio, M.A., Wójtowicz, M.A., Chen, Y., Charpenay, S., Jensen, A, Bassilakis, R., Riek, K., "A Comprehensive Model of Biomass Pyrolysis," Final Report USDA 96-33610-2675, (1997).

15 Carangelo, R.M., Solomon, P.R., and Gerson, D.G., Fuel, 66, 960 (1987).

16 Carangelo, R.M., Solomon, P.R., Bassilakis, R., Gravel, D., Baillargeon, M., Baudais, F., and Vail, G., American Laboratory, P. 51, (1990).

17 Milosavljevic, I., Oja, V. and Suuberg, E.M., "Thermal Effects in Cellulose Pyrolysis-Relationship to Char Formation Processes," I&EC Research, 35, 653-662 (1996).

18 Chen, Y., DiTaranto, M., Kroo, E., Wójtowicz, M.A., Suuberg, E.M., and Serio, M.A., "Pyrolysis Processing for Solid Waste Resource Recovery in Space," Final Report submitted under contract NAS2-99001, June 1999.

19 Serio, M.A., Chen, Y., and Wójtowicz, M., "Pyrolysis Processing for Solid Waste Resource Recovery in Space," Submitted to 30th International Conference on Environmental Systems, Toulouse, France, July 10-13, 2000.

20 Klass, D.L., Biomass for Renewable Energy, Fuels and Chemicals, Academic Press, New York (1988).

PROPERTIES AND POTENTIAL ENVIRONMENTAL APPLICATIONS OF CARBON ADSORBENTS FROM WASTE TIRE RUBBER

Christopher M.B. Lehmann[1,2], David Rameriz[2],
Mark. J. Rood[2], and Massoud Rostam-Abadi[1,2]

[1] Energy and Environmental Engineering Section
Illinois State Geological Survey
Champaign, IL 61820

[2] Department of Civil and Environmental Engineering
University of Illinois at Urbana-Champaign
205 N. Mathews Ave.
Urbana, IL 61801

KEYWORDS: carbon adsorbent, pyrolysis, tire recycling, air pollution

ABSTRACT

The properties of tire-derived carbon adsorbents (TDCA) produced from select tire chars were compared with those derived from an Illinois coal and pistachio nut shells. Chemical analyses of the TDCA indicated that these materials contain metallic elements not present in coal- and nut shell-derived carbons. These metals, introduced during the production of tire rubber, potentially catalyze steam gasification reactions of tire char. TDCA carbons contained larger meso- and macopore volumes than their counterparts derived from coal and nut shell (on the moisture- and ash-free-basis). Adsorptive properties of the tire-derived adsorbent carbons for air separation, gas storage, and gas clean up were also evaluated and compared with those of the coal- and nut shell derived carbons as well as a commercial activated carbon. The results revealed that TDCA carbons are suitable adsorbents for removing vapor-phase mercury from combustion flue gases and hazardous organic compounds from industrial gas streams.

INTRODUCTION

The issue of disposing of waste tires in industrialized nations has become a pervasive issue that requires remedy. Data from a U.S. EPA study in 1993 indicates that 242 million waste tires are generated in the United States each year, corresponding to approximately one tire per US citizen per year[1]. The trend of one tire generated per person-year is generally applicable to industrialized nations. Tire stockpiles have created significant environmental concerns: the open shape of tires allows rainwater to collect, making them ideal breeding grounds for mosquitoes and vermin; tire stockpile fires are of concern since used tires are readily combustible and are difficult to extinguish; and finally, tire stockpiles are an aesthetic concern, since they are frequently located near densely-populated areas where large numbers of tires are generated. The millions of metric tonnes of waste tires are a potential feedstock for the production of new materials. However, data from the U.S. EPA indicates that only ~20% of waste tires are utilized in a given year, and the rest are disposed of in tire stockpiles or landfills; two to three billion tires were stored thusly as of 1993[1].

Pyrolysis has been proposed as a method for decomposing some of the tire rubber to salable oil, gas, and char (principally carbon black). The yield of char from tire pyrolysis is about 30 wt%, which could be upgraded into a value-added tire-derived carbon adsorbent (TDCA). Producing TDCA from waste tires may potentially provide an economic incentive for commercializing tire pyrolysis as a recycling process.

The work presented in this paper summarizes the results from an ongoing collaborative research program between the Illinois State Geological Survey and the University of Illinois at Urban-Champaign to prepare and evaluate the applications of TDCA for gas purification and clean up. TDCA samples were prepared in both laboratory- and pilot-scale reactors. The properties of TDCAs were compared to those derived from a high-sulfur bituminous Illinois coal and pistachio nut shells. These adsorbents were evaluated for removal of vapor-phase mercury species (Hg^0 and $HgCl_2$) from simulated coal combustion flue gases and for capture of gaseous organic solvents, including acetone and methyl-ethyl-ketone (MEK). These compounds are of concern due to their large source strength to the atmosphere (Table 1).

Adsorption processes are widely utilized in air pollution control operations for removing hazardous gases from industrial flue gas streams. A porous solid with large surface area and micropore volume is key for efficient removal of pollutants in any adsorption process. Adsorbents produced from different precursor materials will have differing properties due to inherent variations in the chemical and physical nature of precursor materials.

METHODOLOGY

Carbon adsorbents were prepared by heating the tire, coal, or pistachio shell in a fixed-bed reactor to 850°C under a nitrogen purge. The char was then activated in steam at 850°C. Activation rates of the precursor chars were obtained with a thermogravimetric analyzer (CAHN TG-131) in either a 100% CO_2 or (50% CO_2)/(50% steam) mixture at 850°C. The precursors were analyzed for their moisture, ash, carbon, hydrogen, nitrogen, and total sulfur contents using standard ASTM methodology (Table 2).

The surface structure and morphology of prepared adsorbents were evaluated via nitrogen adsorption (at 77 K) and scanning electron microscopy. Nitrogen adsorption isotherms were determined via an adsorption apparatus (Micromeritics ASAP 2400). Surface areas were determined via the standard BET equation. Total pore volumes were determined at $P/P_0 \approx 0.98$ and micropore volumes were evaluated using the 3-D pore size distribution model developed at ISGS/UIUC.[3] Scanning electron micrographs (SEM) were collected from prepared samples (Amary 1830).

Elemental mercury (Hg^0) and mercuric chloride ($HgCl_2$) equilibrium adsorption capacities for prepared samples were completed by Radian International LLC (Austin, TX). Tests were carried out in a simulated flue gas containing 1600 ppm$_v$ SO_2, 50 ppm$_v$ HCl, 12% CO_2, 7% H_2O, 6% O_2 and 40-60 $\mu g/N\text{-}m^3$ Hg^0 or $HgCl_2$. Adsorption capacities were measured using cold-vapor atomic adsorption. Equilibrium acetone and MEK capacities were determined in a gravimetric analyzer (CAHN 2000) using standardized gas cylinders diluted with nitrogen.

RESULTS AND DISCUSSION

Proximate analyses of the adsorbent precursor materials indicate that the principle differences are in the ash, sulfur, and carbon contents (Table 2). The ash content of pistachio shells is negligible in comparison with coal and tire-based materials. Ash contents are of interest since concentrations of trace species, especially metals, likely influence gasification rates and adsorption properties of materials. Total sulfur contents of precursor adsorbents also differed, again with pistachio having a negligible sulfur content in comparison to the coal and tire precursors. Sulfur contents are of interest, since they likely influence the adsorption of mercury species.

The steam gasification rate (on the total mass basis) of tire char was larger than the coal char (Figure 1). Its CO_2 gasification rate was, however, much smaller than the pistachio char. Properties of select carbon adsorbents prepared in the fixed-bed reactor are presented in Table 3. The data are shown for test conditions that resulted in about 15% yield in adsorbent prepared from tire and pistachio shell, and about 30% yield from the coal. The surface area of the TDCA (389 m^2/g) was about one-half of the coal and pistachio carbons. The TDCA , however, had 32% larger total pore volume (0.670 vs 0.505 cc/g) than the coal and pistachio carbons. Pistachio and coal carbons were more microporous than TDCA; more than 50% of the pores in the coal and pistachio carbons were in the micropore range as compared to 34% for the TDCA. TDCAs with surface areas as large as 1000 m^2/g, and micropore volumes as large as 0.5 cc/g have been prepared (Figure 2). The reactivity and pore structure data suggest that there should not be any difficulties in developing porosity in tire-derived char using steam.

Scanning electron micrographs of the pistachio-derived carbon revealed that it had a more heterogenous and "rougher" surface than coal-derived carbon (Figures 3 and 5). The surface texture of the TDCA was intermediate between the coal and the pistachio-derived carbons (Figure 4) with various rod-like and clusters of matters present on its surface. EDS revealed that the rod-like matters were typically composed of zinc and sulfur species, and that the jagged "globs" were generally composed of calcium and Si. It appears that ZnO (an additive added to tire) is converted to ZnS during the activation of tire char with steam.

Air pollution applications of adsorbents. Coal -derived carbon had the largest capacity (2718 $\mu g/g$) for adsorption of Hg^0 from the simulated coal combustion flue gas followed by tire- (872 $\mu g/g$) and pistachio-derived (500 $\mu g/g$) carbons (Figure 6). The TDCA and pistachio carbon, however, had about five times larger capacity for adsorption of $HgCl_2$ than their coal-derived counterpart. The presence of larger micropore volume and larger concentration of organic sulfur in the coal-derived carbon was potentially responsible for the large Hg adsorption capacity of this sample.[4] Since tire rubber contains organically bound sulfur from the vulcanization process, it could potentially be a suitable precursor for preparing effective Hg adsorbent. Indeed, the results from extensive mercury testing with several TDCAs, using five different compositions of simulated coal combustion flue gas, revealed that TDCA is an effective sorbent for removal of both Hg and $HgCl_2$.[5]

Plots of capacity of TDCA for adsorption of acetone and MEK as a function of the adsorbate concentration (ppm$_v$) at select temperatures are shown in Figure 7. As expected, the adsorption capacity increased with increasing adsorbate concentration, and decreased with increasing temperature. In the case of acetone, the adsorption capacity ranged from 15 to 41 mg/g to 59 to 125 mg/g as temperature varied from 20°C to 50°C. For MEK, the adsorption capacity ranged from 43

to 101 mg/g to 93 to 197 mg/g as temperature varied from 20°C to 50°C. The adsorption of MEK was larger than the adsorption of acetone at the same conditions of temperature and adsorbate concentration. Equilibrium adsorption capacities for acetone were also determined for a commercial carbon (Calgon BPL, surface area = 965 m^2/g) in a previous study.[6] The equilibrium acetone capacities for TDCA was about 70% of the capacity observed for BPL, 225 mg/g at 10000 ppm_v.

CONCLUSIONS

The work presented here showed that carbon adsorbents with adequate surface area and pore volume could be prepared from waste tire rubber. Furthermore, adsorption studies indicated that TDCAs were suitable sorbents for removal of trace amounts of vapor-phase mercury from coal combustion flue gases, and for purification of gas streams containing hazardous organic compounds. Further work is required to identify the potential application of TDCA for other pollution control operations. In addition, research in identifying the roles of various metals in the waste tire during thermal processing, pore structure development, and any catalytic properties during adsorption/desorption processes should be investigated. Finally, the commercial success for producing TDCA depends on the market size and the selling price for both the tire-derived oil and the TDCA.

ACKNOWLEDGMENTS

Support from the Office of Solid Waste Research at the University of Illinois at Urbana-Champaign made this research possible.

REFERENCES

1. Clark, C.; Meardon, K.; Russell, D., *Scrap Tire Technology and Markets*; Pollution Technology Review No. 2ll; U.S. Environmental Protection Agency: Park Ridge, NJ, 1993.
2. U.S. Environmental Protection Agency; *Toxic Release Inventory*; TRI Explorer; http://www.epa.gov/triexplorer/reports.htm.
3. Sun, J.; Chen, S.; Rood, M.J.; Rostam-Abadi, M.; *Energy & Fuels*; **1998**; *12*, 1071.
4. Hsi, H.C.; Chen, S.; Rostam-Abadi, M.; et al.; *Energy & Fuels*; **1998**; *12*, 1061.
5. ***Development and Evaluation of Low Cost Mercury Sorbents***, EPRI, Palo Alto, CA: TE-114043.
6. Lehmann, C.M.B.; Rostam-Abadi, M.; Rood, M.J.; Sun, J.; *Energy & Fuels*; **1998**; *12*, 1095.

Table 1. Total air emissions (million kg per year), 1988-1998.

	1988	1989	1990	1991	1992	1993	1994	1995	1996	1997	1998
MEK	64.3	63.9	61.2	49.6	42.5	39.4	36.4	31.9	27.4	24.2	21.1
acetone	96.5	96.2	88.5	74.3	63.4	59.0	---	---	---	---	---
mercury	0.010	0.011	0.010	0.008	0.006	0.005	0.005	0.006	0.006	0.006	0.006

Source: U.S. EPA (http://www.epa.gov/triexplorer/trends.htm)
Note: Acetone removed from TRI in 1994

Table 2. Properties of raw sorbent materials.

	coal	raw tire	tire char	pistachio shell
moisture	9.3	0.5	0.3	4.4
ash[a]	11.5	3.0	15.4	0.2
carbon[a]	68.1	87.2	78.8	48.0
hydrogen[a]	4.8	7.6	0.8	6.1
nitrogen[a]	1.2	0.2	0.2	0.1
oxygen[a,b]	10.5	0.9	2.0	45.5
total sulfur[a]	3.7	1.6	2.9	0.2

[a] moisture-free values
[b] oxygen content determined by difference

Table 3. Properties of prepared adsorbents.

	coal	tire	pistachio shell
ash [wt. %]	27.0	---	---
sulfur content	1.6	---	---
yield [%]	30.0	14.7	14.8
surface area [m^2/g]	787	389	775
total pore volume [cc/g]	0.504	0.670	0.505
micropore volume [cc/g]	0.265	0.230	0.312

— = not measured

Figure 1. Gasification rate of select precursor materials in CO_2 or steam/CO_2 mixture at 850°C.

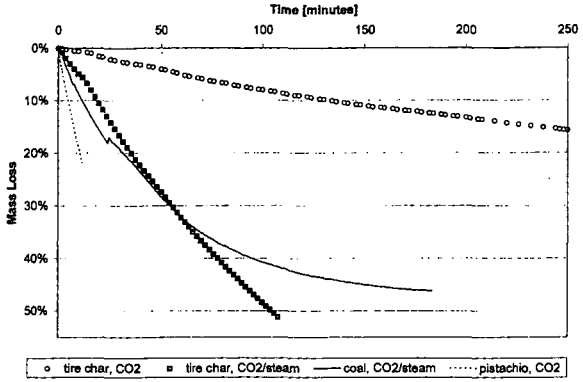

Figure 2. (A) BET-N_2 surface area and (B) micropore volume vs. yield for TDCA.

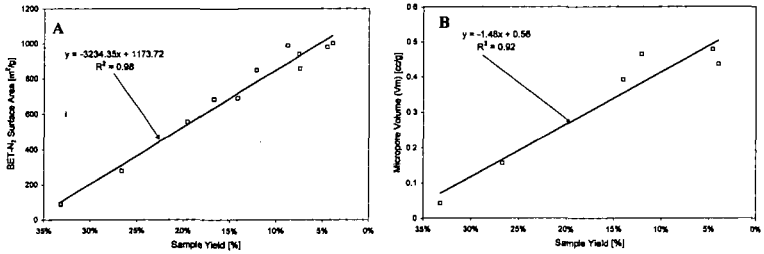

Figure 3. SEM of Illinois coal-derived adsorbent (4780x magnification).

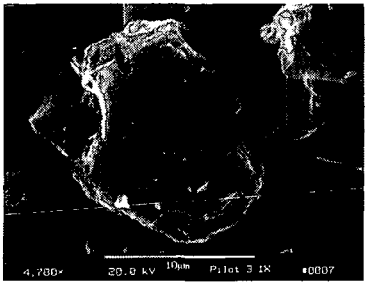

Figure 4. SEM of tire-derived adsorbent (3800x magnification).

Figure 5. SEM of pistachio shell-derived adsorbent (3800x magnification).

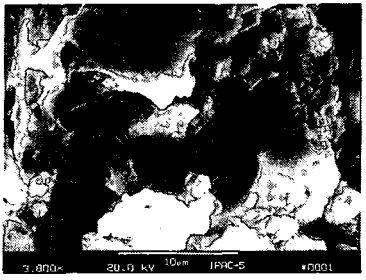

Figure 6. Hg^0 and $HgCl_2$ equilibrium capacities of adsorbents at 135°C.

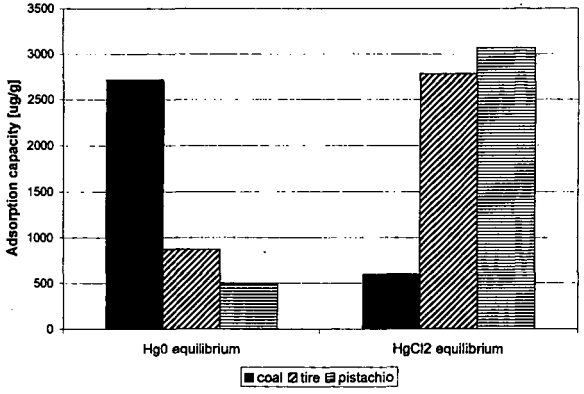

Figure 7. (A) Acetone and (B) MEK capacities of TDCA at 20-50°C.